Journal of the Korean Nuclear Society
Volume 35, Number 6, pp.537~546, December, 2003

Buckling Characteristics of the KALIMER-150 Reactor Vessel Under Lateral Seismic Loads and the Experimental Verification Using Reduced Scale Cylindrical Shell Structures

Gyeong-Hoi Koo and Jae-Han Lee
Korea Atomic Energy Research Institute,
150 Dukjin-dong, Yuseung-gu, Daejeon 305-353, Korea
ghkoo@kaeri.re.kr

(Received May 29, 2003)

Abstract

The purpose of this paper is to investigate the buckling characteristics of a conceptually designed KALIMER-150(Korea Advanced LIquid MEtal Reactor, 150MWe) reactor vessel and verify the buckling behavior using the reduced scale cylindrical shell structures. To do this, nonlinear buckling analyses using finite element method and evaluation formulae are carried out. From the results, the KALIMER-150 reactor vessel exhibits a dominant bending buckling mode and is significantly affected by the plastic behavior. The interaction effects with the vertical seismic load cause the lateral buckling load to be slightly decrease. From the results of the buckling experiments using reduced scaled cylindrical shell structures, it is verified that the buckling modes such as pure bending, pure shear, and mixed(bending plus shear) mode clearly appear under a lateral load corresponding to the slenderness ratio of cylinder.

Key Words : KALIMER-150, buckling analysis, buckling experiment, buckling load, buckling mode, seis mic load

1. Introduction

Compared with conventional PWRs, the liquid metal reactor(LMR) has so different design characteristics in operating temperatures over 500 ℃ and lower pressures under 5bar. Because of these design characteristics, the reactor vessel is designed to be a relatively very thin-walled cylindrical shell structure to prevent a large thermal gradient invoking severe thermal stress. Therefore, buckling design of a thin reactor vessel of a LMR is one of the main structural integrity issues for the LMR[1~5].

In this paper, the analyses of the buckling characteristics under a lateral seismic load for the preliminary designed KALIMER-150(Korea Advanced LIquid MEtal Reactor, 150MWe) reactor vessel[6] are carried out using three types of finite element analyses, eigenvalue buckling analysis, nonlinear elastic buckling analysis, and nonlinear

elastic-plastic buckling analysis and the results are compared with those of the evaluation formulae proposed by Okada and his colleague[7]. The effects of a vertical seismic load on the buckling characteristics are investigated with considerations of the pre-stressed tension or compression load in a lateral buckling analyses. To consider material degradation due to the elevated operation temperature and the structural damages such as the ratcheting deformation and creep-fatigue damage during the total service life time of 30 years, the method using the isochronous stress-strain curve for the design material at the specified temperature and hold time provided in the ASME B&PV Section III, Subsection NH[8] is proposed in the nonlinear buckling analyses.

To verify the buckling characteristics under a lateral seismic load, experimental buckling tests are carried out with reduced scale cylindrical shell structures having various slenderness ratios. The dimensions of the test cylinders are determined to have the bending, shear, and mixed buckling modes evaluated by the formulae. The buckling characteristics by the numerical simulation results are verified by comparison with the test results.

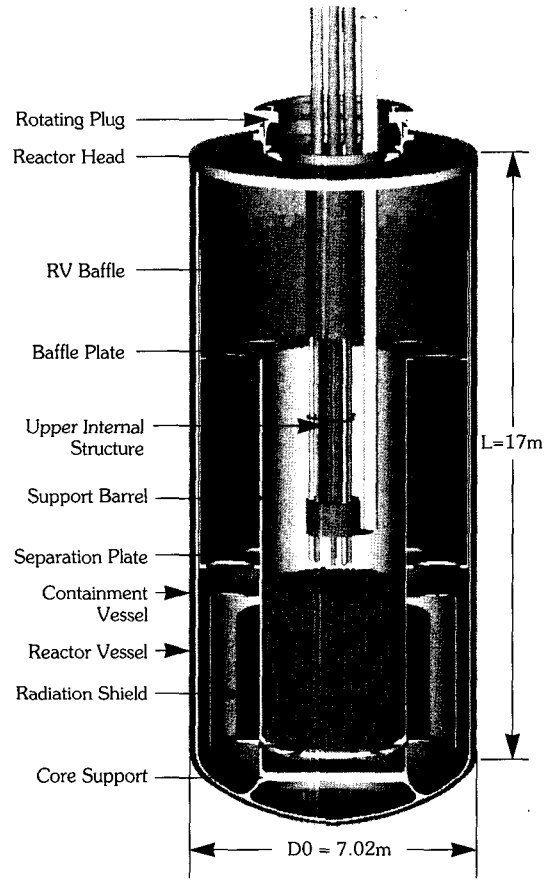

Fig. 1. Conceptually Designed KALIMER-150 Reactor Structures

2. Buckling Characteristics of KALIMER-150 Reactor Vessel

2.1. Descriptions of Reactor Vessel

Fig. 1 shows the conceptually designed KALIMER-150 liquid metal reactor. As shown in figure, the KALIMER reactor vessel is a very thin and long structure compared with a conventional PWR. The length of the side cylinder is 1700cm and the outer diameter is 702cm. The thickness of the reactor vessel is 5cm, which is very small compared with about 25cm of the conventional PWR. Most of the reactor internal structures and fuel assemblies are supported by the simple skirt structure welded to the reactor vessel's bottom head. Therefore, the reactor vessel will act as the cantilever structure and be subjected to the force at the end of the lateral seismic load.

2.2. Numerical Buckling Simulation Methods

2.2.1. by Finite Element Methods

There are two types of finite element methods to be used in the buckling analysis. One is the eigenvalue buckling analysis and the other is the nonlinear buckling analysis.

Eigenvalue buckling analysis predicts the

theoretical buckling strength(the bifurcation point) of an ideal linear elastic structure. Bifurcation buckling refers to the unbounded growth of a new deformation pattern. The buckling problem is formulated as an eigenvalue problem as follows:

$$([K] + \lambda_i [S])\{\psi\}_i = \{0\}, \quad (1)$$

where the matrices [K] and [S] indicate the system stiffness matrix and the stress stiffness matrix respectively, λ_i is the ith eigenvalue, and $\{\psi\}_i$ is the ith eigenvector of displacements. The eigenvectors are normalized so that the largest component is 1.0. Imperfections and material nonlinearities cannot be included in this analysis. Thus, the buckling strength obtained by the eigenvalue buckling analysis may differ from that of a real structure and often yields unconservative results. Therefore, care is needed when using this method in the actual evaluation of buckling strength.

Nonlinear buckling analysis including geometric and material nonlinearities is usually the more accurate approach and is therefore recommended for the design or evaluation of actual structures. There are two methods for obtaining buckling strength by nonlinear buckling analysis. One basic approach is to constantly increment the applied loads until the solution begins to diverge, which can be obtained from the load-controlled buckling analysis. In this approach, a simple static analysis will be done with large deflections extended to a point where the structure reaches its limit load. Another approach is to constantly increment the displacement sufficient to obtain the snap-through buckling curve, which can be obtained from the displacement-controlled buckling analysis. In a nonlinear buckling analysis, a sufficiently fine load or displacement increment should be used to obtain the expected buckling strength.

2.2.2. by Evaluation Formulae

The buckling strength of a cylindrical shell structure under shear force can be obtained on the basis of the theoretically calculated elastic buckling loads. By including the effects of the initial geometrical imperfections and plasticity, the critical shear buckling load which causes buckling of a cylindrical shell can be represented as :

$$Q_{cr} = \alpha \, Min[\, Q^b_{cr,o} \, , \, Q^s_{cr,o} \,], \quad (2)$$

where α is the imperfection reduction factor. $Q^b_{cr,o}$ and $Q^s_{cr,o}$ in Eq. (2) represent the critical shear loads which induce elastic-plastic bending buckling and shear buckling respectively. These critical shear loads can be represented as follows:

$$Q^b_{cr,o} = y_b \, \eta_c \, Q^b_{cr,e}, \quad (3)$$

$$Q^s_{cr,o} = y_s \, \eta_s \, Q^s_{cr,e}. \quad (4)$$

In Eq. (3) and Eq. (4), $Q^b_{cr,e}$ and $Q^s_{cr,e}$ represent the theoretical elastic bending and the shear buckling load for a perfect shape of a cylindrical shell, respectively, η_c and η_s represent the plasticity reduction factors for axial compressive buckling and shear buckling, respectively, and y_b and y_s represent the axial and the shear stress distribution factors, respectively. These factors can be determined analytically as functions of the following geometric and material parameters of a cylindrical shell: R(radius), t(thickness), L(length), E(Young's modulus), $\sigma_{0.2}$(0.2% proof stress) and ν(Poisson's ratio). For LMR component materials such as 304SS, 316SS and Mod.9Cr-1Mo steel, these factors can be obtained approximately by the assumption of a Ramberg-Osgood type stress-strain relation as follows[7]:

$$\eta_c = Min[1.0, 1.04 \tanh(0.98 \sigma_{0.7E} / \sigma^c_{cr,e})], \quad (5)$$

$$\eta_s = Min[1.14\tanh(\tau_{0.7E}/\tau^s_{cr,e}), \tanh(1.6\tau_{0.7E}/\tau^s_{cr,e})], \quad (6)$$

$$y_b = 1.0+0.21\,\mathrm{sech}(3.5\sigma_{0.7E}/\sigma^c_{cr,e}), \quad (7)$$

$$y_s = Min[1.0+0.22\,\mathrm{sech}(1.7\tau_{0.7E}/\tau^s_{cr,e}), 1.0+13.0\,\mathrm{sech}(6.4\tau_{0.7E}/\tau^s_{cr,e})], \quad (8)$$

where

$$\sigma_{0.7E} = 1.815E^{-1/9}\sigma_{0.2}^{10/9}, \quad (9)$$

$$\tau_{0.7E} = \sigma_{0.7E}/\sqrt{3}\ . \quad (10)$$

In Eqs.(5)~(8), $\sigma^c_{cr,e}$ and $\tau^s_{cr,e}$ are theoretical elastic buckling stresses for axial compression and shear, respectively, and can be expressed as [9,10]:

$$\sigma^c_{cr,e} = [3(1-\nu^2)]^{-1/2}\frac{Et}{R}, \quad (11)$$

$$\tau^s_{cr,e} = 0.07708\frac{\pi^2 E}{(1-\nu^2)^{5/8}}\left(\frac{R}{t}\right)^{-5/4}\left(\frac{L}{R}\right)^{-1/2}. \quad (12)$$

For the effects of any initial geometrical imperfections on the buckling strength, an imperfection similar to the buckling mode is known as the most severe geometrical shape reducing the buckling strength[3]. In this paper, the imperfection reduction factor, α in Eq. (2) developed by Okada etc. is used as follows:

$$\alpha = 0.66\gamma^2 - 0.9\gamma + 1.0\ , \quad (13)$$

where

$$\gamma = \frac{\sigma_{0.2}}{E}\frac{R}{t}\ . \quad (14)$$

The applicable dimensional ranges of the cylindrical shell for the evaluation formulae of buckling strength are $0.5 < L/R < 5.0$ and $50.0 < R/t < 500.0$.

2.3. Analyses of Buckling Characteristics

For the numerical simulation, the commercial finite element computer program, ANSYS version 5.6[11] is used. In this paper, three types of buckling analyses, eigenvalue buckling analysis, nonlinear elastic buckling analysis, and nonlinear elastic-plastic buckling analysis are carried out. Fig. 2 shows a half symmetric 3D finite element analysis model using a 4-node elastic shell element(SHELL63) for the eigenvalue and nonlinear buckling analysis without the plasticity effect and a 4-node plastic large strain shell

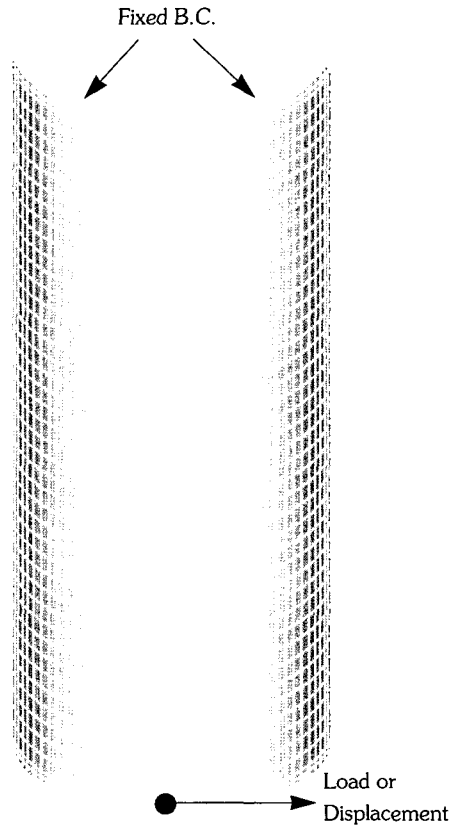

Fig. 2. Finite Element Analysis Model of KALIMER-150 Reactor Vessel (Half Symmetry)

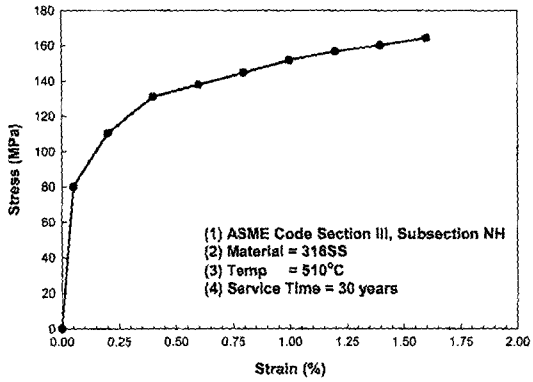

Fig. 3. Stress-Strain Curve Used in Nonlinear Elastic-Plastic Buckling Analysis

element(SHELL43) for the nonlinear buckling analysis with plasticity effect. In the buckling analyses, it is assumed that the total lateral seismic load induced by the inertia mass of the core and the reactor internal structures is applied to the bottom end of the side cylinder conservatively as shown in Fig. 2. The isochronous stress-strain curve corresponding to the service lifetime of 30 years and the assumed average metal temperature for a normal operation, 510℃, provided in ASME Subsection NH, is used in the nonlinear buckling analysis as shown in Fig. 3.

The input parameters used in the calculation of the critical buckling load by the evaluation formulae are: L/R=4.88, R/t=69.7, E=160GPa, $\sigma_{0.2}$=120.0MPa, ν=0.3.

2.3.1. Results : No vertical Seismic Load

Fig. 4 shows the results of the buckling mode obtained by each analysis method. As shown in the figure, all the methods present the same bending buckling mode as dominant in the KALIMER-150 reactor vessel. Due to the large slenderness ratio of the reactor vessel, L/R=4.88, significant axial compressive stress occurs at the fixed boundary region due to the bending buckling moment and causes bending buckling deformation.

The results of the critical buckling load obtained from the evaluation formulae and the numerical simulations for the KALIMER-150 reactor vessel are as follows:

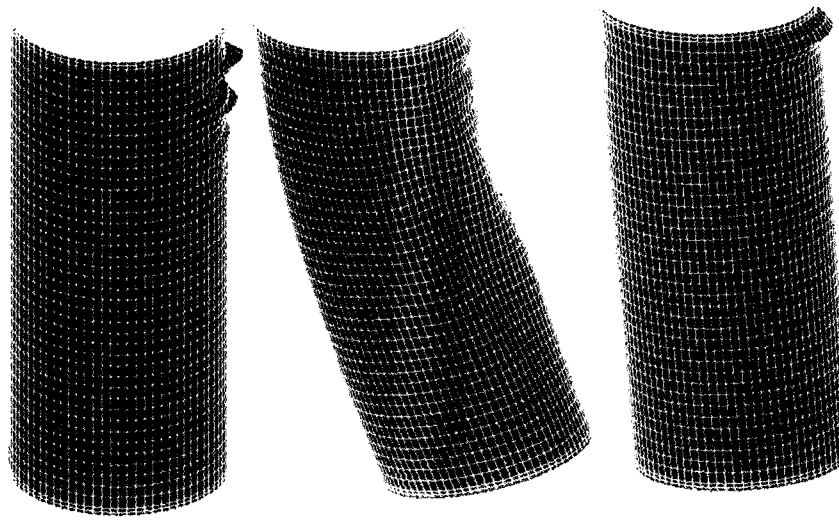

(c) Eigenvalue Buckling Analysis

(b) Nonlinear Elastic Buckling Analysis

(a) Nonlinear Elastic-Plastic Buckling Analysis

Fig. 4. Buckling Mode Shapes of KALIMER-150 Reactor Vessel

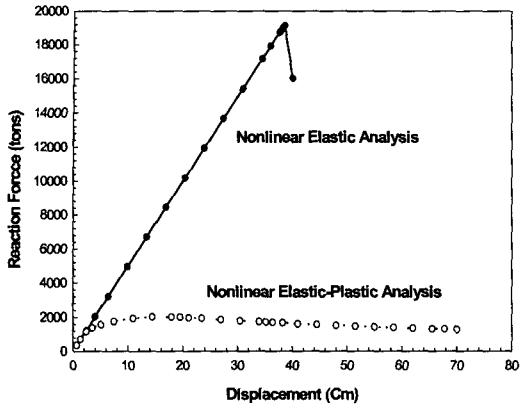

Fig. 5. Load-Displacement Curves of KALIMER-150 Reactor Vessel

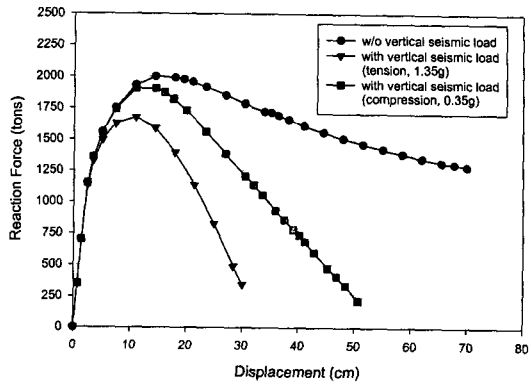

Fig. 6. Effects of Vertial Seismic Loads on Load-Displacement Curves of KALIMER-150 Reactor Vessel

- Evaluation formulae : Q_{cr} = 12.94 MN (bending mode),
- Eigenvalue analysis : Q_{cr} = 311.92 MN (bending mode),
- Nonlinear elastic analysis : Q_{cr} = 188.67 MN (bending mode),
- Nonlinear elastic-plastic analysis : Q_{cr} = 19.60 MN(bending mode).

From the results of the critical buckling load obtained from the nonlinear buckling analyses, it appears that plasticity behavior significantly affects the buckling strength and reduces the critical buckling load. Fig. 5 shows the reaction force-displacement curves calculated by the nonlinear buckling analyses with and without the plasticity effect.

2.3.2. Results : with vertical Seismic Load

To evaluate the buckling characteristics under seismic events, it is necessary to consider not only the horizontal and vertical seismic loads separately but also their interaction.

In this paper, the effects of the vertical seismic load on the lateral seismic buckling problem are investigated for two types axial pre-stresses. One is the axial tension pre-stress and the other one is the axial compression pre-stress. The axial pre-stress used in the analysis is calculated with the assumption of a total reactor weight of 1228 tons and 1.35g for a tension, 0.35g for compression and applied to the free end of the side cylinder[12].

Fig. 6 reveals the analysis results of the load-displacement curve. The results of the critical buckling loads are as follows:

- Without vertical seismic load : Q_{cr} = 19.60 MN,
- With vertical seismic load(compression) : Q_{cr} = 18.67 MN,
- With vertical seismic load(tension) : Q_{cr} = 16.40 MN.

From the results, the buckling load has a slight reduction of about 5% in the case of the vertical compression load and 16% in the case of the vertical tension load than in the case of no vertical seismic load. When the vertical compression load is added, the buckling mode is the same as the case of no vertical load. However, the buckling mode is very different, as shown in Fig. 7, when the vertical tension load is added.

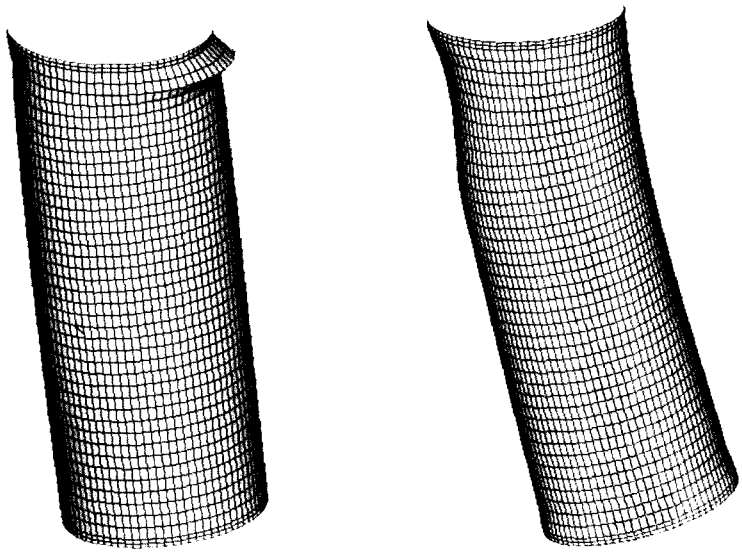

(a) with vertical compression load (b) with vertical tension load

Fig. 7. Buckling Modes with Effects of Vertical Seismic Load

4. Experimental Verification of Buckling Behavior

Experimental buckling tests were performed to verify the buckling characteristics obtained from the numerical simulation methods used in this paper. To do this, the buckling strength evaluations were carried out using the evaluation formulae in section 2.2.2 and three types of reduced scale cylindrical shell structures were determined as shown in Table 1. Each test model was designed to have bending buckling (Model-A, L/R=3.1), bending plus shear(Model-B, L/R=1.6), and shear buckling(Model-C, L/R=1.0). Material properties were close to 304 stainless steel with E = 194GPa, ν=0.27, $\sigma_{0.2}$=250MPa at room temperature. As shown in the fabricated test shell structure, the outer and inner surfaces of the shell top end were connected to the rigid fixtures to provide boundary conditions close to the fixed end, and the shell bottom end was connected to rigid fixtures to provide a connecting point with a horizontal hydraulic actuator.

Fig. 8 shows a schematic of the experimental

Table 1. Dimensions of Cylindrical Shell Structures for Buckling Experiments

	Model-A (Bending)	Model-B (Bending+Shear)	Model-C (Shear)
L(mm)	160.0	80.0	50.6
D(mm)	103.0	103.0	103.0
t(mm)	0.5	0.5	0.5
(L/R)	3.1	1.6	1.0

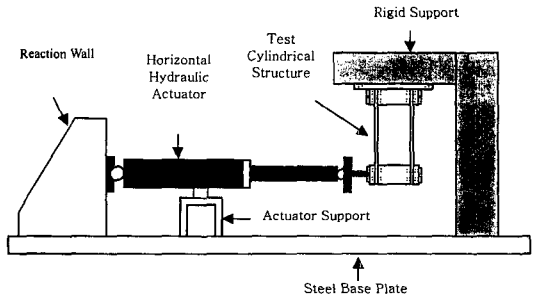

Fig. 8. Schematic of Lateral Buckling Test Facility

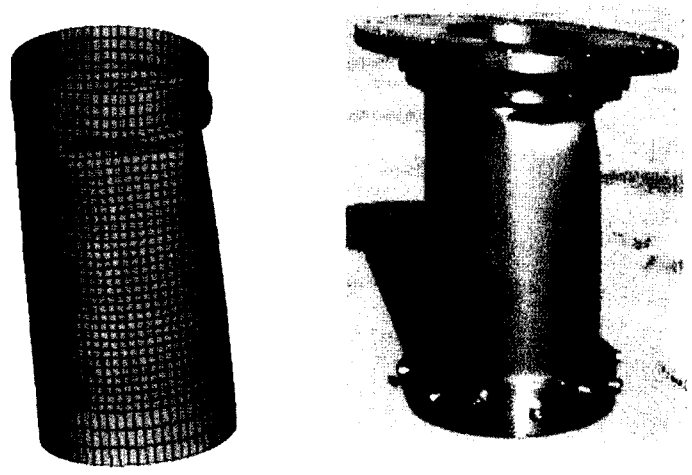

(a) Model-A

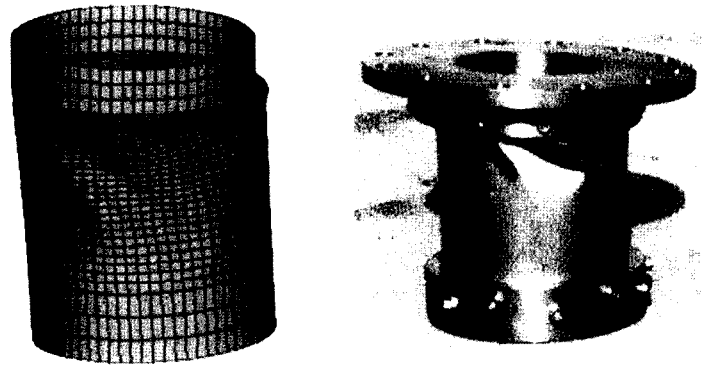

(b) Model-B

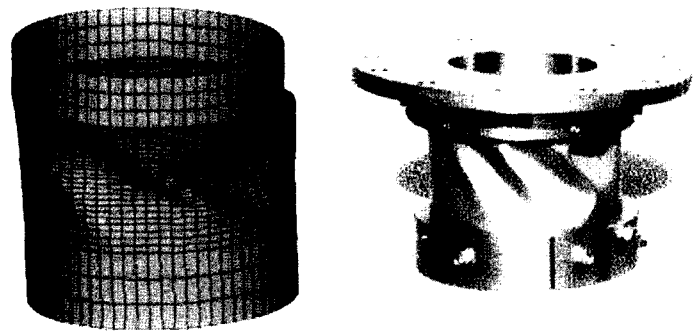

(c) Model-C

Fig. 9. Buckling Modes Shapes for Analyses and Experiments

test machine. The top of the test structure is clamped to a rigid support structure and the bottom is connected to a horizontal hydraulic actuator, which applies a controlled displacement

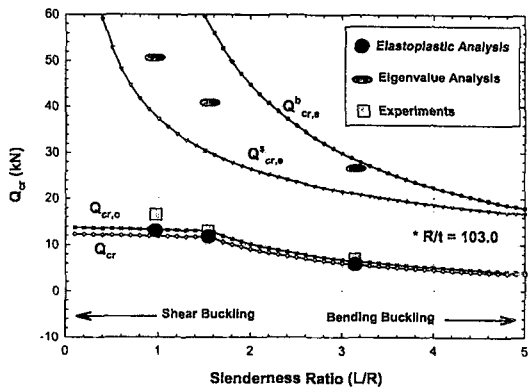

Fig. 10. Comparison of Buckling Loads Corresponding to Slenderness Ratio by Formulae, Analyses and Experiments

load, with a small and rigid connecting bar.

Fig. 9 compares the results of the buckling shapes between the nonlinear elastic-plastic buckling analyses and the experiments after applying a quasi-static 20mm displacement load. From the results, the buckling modes obtained by the numerical simulation are in very good agreement with those of the experiments and it is verified that all the test models reveal very well-expected buckling modes as assumed in the design stage; pure bending mode for Model-A, mixed mode for Model-B, and pure shear mode for Model-C.

Fig. 10 compares the results for the critical buckling loads from the experiments and numerical simulations. In the figure, the solid lines with symbols are the results by the evaluation formulae for the slenderness ratio throughout from 0.1 to 5.0. As shown in figure, it is clearly verified that the elastic buckling loads calculated by the eigenvalue analysis and the evaluation formulae significantly overestimate the critical buckling load compared with those of the experiments. However, the elastic-plastic buckling loads are much smaller than the elastic buckling loads and the results by numerical simulations are in good agreement with the results of the experiments and evaluation formulae. This means that the plastic behavior of the LMR reactor vessel significantly affects the critical buckling load in the lateral seismic loads. Therefore, it is recommended that the nonlinear elastic-plastic buckling analysis should be used in the LMR buckling evaluations.

5. Conclusions

In this paper, buckling characteristics of the KALIMER-150 reactor vessel under a lateral seismic load were investigated using numerical simulations and the evaluation formulae. From the results, the KALIMER-150 reactor vessel exhibits a dominant bending buckling mode and is significantly affected by the plastic behavior. For the interaction effects with the vertical seismic load, it was revealed that the lateral buckling load was slightly reduced by axial tension and compression pre-stress but the buckling mode shapes were different to each other. From the results of the buckling experiments using reduced scaled cylindrical shell structures, it was verified that the buckling modes such as pure bending, pure shear, and mixed(bending plus shear) mode clearly appear under a lateral load corresponding to the slenderness ratio of cylinder.

Acknowledgements

This work has been carried out under the Nuclear R&D Program by MOST in Korea.

Nomenclatures

A_p	maximum seismic peak acceleration response
E	Young's modulus
g	acceleration of gravity
$[K]$	system stiffness matrix

L	length of cylindrical shell
M	total seismic inertia mass
R	radius of cylindrical shell
Q_{cr}	critical bucking load
$Q^b_{cr,o}$, $Q^s_{cr,o}$	critical shear loads inducing bending and shear buckling
$Q^b_{cr,e}$, $Q^s_{cr,e}$	theoretical elastic bending and shear buckling loads
Q_d	design or expected seismic load
[S]	stress stiffness matrix
t	thickness of cylindrical shell
y_b, y_s	axial and shear stress distribution factor
α	imperfection reduction factors
λ_i	th eigenvalue
η_c , η_s	plasticity reduction factors
υ	Poisson's ratio
$\sigma_{0.2}$	0.2% proof stress
$\sigma_{cr,e}$, $\tau_{cr,e}$	theoretical elastic buckling stresses for axial compression and shear
$\{\psi\}_i$	ith eigenvector

References

1. K. Tsukimori, "Analysis of the Effects of Interaction between Shear and Bending Load on the Buckling Strength of Cylindrical Shells," Nuclear Engineering and Design, Vol.165, pp.111-141, (1996).
2. H. Nakamura, H. Ohtsubo, et al., "Outline of the Seismic Buckling Design Guideline of FBR-Tentative Draft-, SMiRT 11 Transactions Vol. E, pp.239-250, (1991).
3. T. Murakami, H. Yoguchi, et al, "The Effects of Geometrical Imperfection on Shear Buckling Strength of Cylindrical Shells," Proc. SMiRT-11, Vol. E., (1991).
4. S. Matsuura, H. Nakamura, et.al., "Buckling Strength Evaluation of FBR Main Vessels under Lateral Seismic Loads," 11 Transactions Vol. E, pp.269-280, (1991).
5. G. H. Koo and J.H. Lee, "Buckling Analyses and Tests for Thin Cylindrical Structures Subjecting the Shear Loads," Proceeding of the Korean Nuclear Society Spring Meeting, (2003).
6. Han DH, Koo GH, et al. KALIMER conceptual design report, Korea Atomic Energy Research Institute. KAERI/TR-2204/(2002, 2002).
7. J. Okada, K. Iwata, et al., "An Evaluation Method for Elastic-Plastic Buckling of Cylindrical Shells under Shear Forces," Nuclear Engineering and Design, Vol.157, pp.65-79, (1995).
8. ASME Boiler and Pressure Vessel Code Section III, Subsection NH, (1995).
9. S.P. Timoshenko et al., Theory of Elastic Stability, McGraw-Hill, 2nd edn., (1961).
10. N. Yamaki, Elastic Stability of Circular Cylindrical Shells, North-Holland Series in Applied Math. And Mech., (1984).
11. ANSYS User's Manual for Revision 5.6, Volume I, II, III.
12. G.H. Koo, H.Y. Lee, B. Yoo, "Seismic Design and Analysis of Seismically Isolated KALIMER Reactor Structures," Journal of the Earthquake Engineering Society of Korea, Vol.3, No.1, pp.75-92, (1999).